ENHANCED RADAR DETECTION AND RANGE ESTIMATION VIA OVERSAMPLED DATA

Augusto Aubry
CNR, IREA
via Diocleziano
328, I-80124
Napoli, Italy
aubry.a@irea.cnr.it

Antonio De Maio
Università di Napoli
"Federico II" DIETI
Via Claudio 21, I-80125
Napoli, Italy,
ademaio@unina.it

Goffredo Foglia, Danilo Orlando
ELETTRONICA S.p.A.
Via Tiburtina Valeria
Km 13,700, 00131 Roma
goffredo.foglia@gmail.com
danilor78@gmail.com

Chengpeng Hao
Institute of Acoustics,
Chinese Academy
of Sciences,
100190 Beijing, China
haochengp@mail.ioa.ac.cn.

ABSTRACT

In this work we propose an adaptive receiver with enhanced range estimation capabilities, which jointly exploits the oversampling of the noisy returns and the spillover of target energy to adjacent range samples. To this end, a proper discrete-time model for the received signal is introduced. Then, the Generalized Likelihood Ratio Test (GLRT) is derived and assessed. The performance analysis highlights that better detection performances and increased range estimation accuracies can be achieved exploiting the oversampling at the price of an additional processing cost.

Index Terms— Adaptive Radar Detection, Constant False Alarm Rate (CFAR), Generalized Likelihood Ratio Test (GLRT), Range Estimation, Oversampling.

1. INTRODUCTION

Adaptive radar detection of point-like or extended targets embedded in Gaussian disturbance represents an active field of research, wherein the seminal paper by Kelly [1] and the technical report [2] are considered points of reference. Indeed, most recent papers rely on the results contained in the above works. Specifically, in [1] Kelly resorts to the Generalized Likelihood Ratio Test (GLRT) to derive a Constant False Alarm Rate (CFAR) test for detecting signals known up to a scaling factor. In [2] a more general framework for adaptive detection has been proposed. Other different solutions can be found in open literature (see for instance [3]). The reader is referred to [4] for a list of papers concerning detection of radar targets against ground and sea clutter, clustered according to several related issues.

Most detectors considered so far assume that the target is located exactly "where the matched filter is sampled" and, hence, that there is no straddle loss, namely no spillover of target energy to adjacent matched filter returns. While this is a reasonable approach, it does not fully use the information provided by the measurements from the two sampling points and, hence, does not share optimality properties [5]. In [5] it is assumed that several closely spaced targets fall within the same beam of a monopulse radar and among three or more adjacent matched filter samples in range; for the considered scenario a Maximum Likelihood (ML) extractor is developed that makes use of monopulse information from the above samples to estimate the angles and ranges of the targets. This idea is further investigated in order to estimate the angles and ranges of multiple unresolved extended targets in [6]. In [7], the authors focus on space-time adaptive processing [8, 9] and devise decision schemes for point-like targets which suitably exploit the spillover of target energy to provide accurate estimates of the target position within the CUT (sub-bin accuracy). The range gates are formed by sampling the output of a filter matched to the transmitted pulse, $p(t)$ say, every T_p seconds with T_p the duration of $p(t)$. Moreover, it is also shown that decision schemes conceived to detect distributed targets, see [2, 10, 11, 12], can be used to account for the spillover of a point-like target.

In the present work, we focus on the same framework as [7] and derive an adaptive receiver capable of ensuring better detection and range estimation performances than those proposed in [7] at the price of an additional processing cost. To this end, we suitably oversample the output of the pulse matched filter coming up with a modified discrete-time model of the received signal. As a consequence, the number of data vectors to be processed and associated with the same range gate is increased by a factor depending on the sampling rate. Then, we apply the GLRT design criteria to obtain a decision scheme jointly processing the vectors associated with the same CUT. Remarkably, the newly proposed architecture guarantees the CFAR property with respect to the unknown parameters of the disturbance.

The remainder of the paper is organized as follows. Next section is devoted to the problem formulation and describes the discrete-time signal and interference models. Section 3 focuses on the design of the detector while Section 4 provides illustrative examples. Section 5 contains some concluding remarks.

978-1-4799-2893-4/14/$31.00 ©2014 IEEE

2. PROBLEM FORMULATION

This section is devoted to the description of the discrete-time signal model, assuming a sampling rate greater than the useful signal bandwidth. To this end, let us consider a linear array of N_a identical and uniformly distributed sensors with d the interelement spacing. For the sake of simplicity, we suppose that the array is looking broadside, and, hence, that each sensor transmits the following coherent burst of pulses

$$\Re e \left\{ A e^{j\varphi} \sum_{n=1}^{N_p} p(t-(n-1)T) e^{j2\pi f_c t} \right\}, \quad t \in [0, N_p T) \tag{1}$$

where $\Re e\{z\}$ indicates the real part of the complex number z, $A > 0$ is an amplitude factor related to the transmitted power and $\varphi \in [0, 2\pi)$ is the initial phase of the carrier signal, $p(t)$ is a unit-energy rectangular pulse waveform of duration T_p and one-sided bandwidth $W_p \approx 1/T_p$, N_p is the number of pulses contained in a coherent processing interval and T is the pulse repetition time, $f_c = c/\lambda$ is the carrier frequency with c the velocity of propagation in the medium and λ the carrier wavelength. The signal backscattered from a target is down converted to baseband and passes through a filter matched to $p(t)$. The output of this filter for the ith sensor is given by (for further details we refer the reader to [7, 8])

$$\begin{aligned} z_i(t) = {} & \alpha e^{j2\pi(i-1)\nu_s} \sum_{n=1}^{N_p} \chi_p(t-(n-1)T-\tau, f) \\ & \times e^{j2\pi(n-1)\nu} + n_i(t), \qquad i = 1, \ldots, N_a, \end{aligned} \tag{2}$$

where $\chi_p(\cdot,\cdot)$ is the (complex) ambiguity function of the pulse waveform $p(t)$ [13], $\alpha \in \mathcal{C}$ is a factor which accounts for $Ae^{j\varphi}$, the effects of the transmitting antenna gain, the radiation pattern of the array sensors, the two-way path loss, the radar cross section of the target, etc., τ is the round-trip delay of the received signal, $\nu = fT$, with $f \ll W_p$ the Doppler frequency shift induced by the target (i.e., $f = \frac{2v}{c} f_c$), ν_s is the target normalized spatial frequency, i.e., $\nu_s = (d/\lambda)\cos\psi$, with ψ the polar angle of the target, $n_i(t)$ is the interference component.

The discrete-time form of the signal received at the ith sensor is obtained by sampling $z_i(t)$ at the following time instants

$$t_{l,n} = t_{\min} + (l-1)T_p/N_s + (n-1)T,$$

with $n = 1, \ldots, N_p$, $l = 1, \ldots, L$, where $N_s \in \mathbb{N}$, $t_{\min}$ denotes the beginning of the sampling process, $L \in \mathbb{N}$ is the number of range (sub-)gates representative of the surveillance area, and l is an integer indexing range (sub-)gates according to the value of N_s. Recall that the range resolution[1] is given by $cT_p/2$ and, hence, if $N_s = 1$ then index l accounts for the entire range cell; on the other hand, if $N_s > 1$ then each range cell encompasses several sub-bins (whose number depends on the value of N_s). Finally, the vector of the noisy returns representing the lth range "sub-cell" is obtained grouping the time samples as follows

$$\begin{aligned} \boldsymbol{z}_l^c &= \left[z_1(t_{l,1}) \ldots z_{N_a}(t_{l,1}) \ldots z_1(t_{l,N_p}) \ldots \; z_{N_a}(t_{l,N_p}) \right]^T \\ &= \boldsymbol{s}_l + \boldsymbol{n}_l^c, \end{aligned}$$

where $\boldsymbol{s}_l \in \mathbb{C}^{N\times 1}$ and $\boldsymbol{n}_l^c \in \mathbb{C}^{N\times 1}$ are the signal and the interference components, respectively, with $N = N_a N_p$. Thus, given the *sample under test*, $\boldsymbol{z}_{l_0}^c$ say[2], the detection problem at hand is tantamount to deciding between the H_0 hypothesis that $\boldsymbol{z}_{l_0}$ contains interference only and the alternative hypothesis that it also contains a useful target signal aligned with $\boldsymbol{v}$. In the latter case, in order to exploit the energy spillover in adjacent range samples for localization purposes, we have to account for either $\boldsymbol{z}_{l_0-N_s}^c, \ldots, \boldsymbol{z}_{l_0-1}^c, \boldsymbol{z}_{l_0+1}^c, \ldots, \boldsymbol{z}_{l_0+N_s-1}^c$ or $\boldsymbol{z}_{l_0-N_s+1}^c, \ldots, \boldsymbol{z}_{l_0-1}^c, \boldsymbol{z}_{l_0+1}^c, \ldots, \boldsymbol{z}_{l_0+N_s}^c$ depending on the value of the residual delay $\epsilon \in \mathcal{I} = [-T_p/(2N_s),\, T_p/(2N_s)]$ evaluated with respect to the l_0th range sub-bin.

Before proceeding further, it is worth to underline that, under reasonable technical assumptions, the structure of the fast-time interference correlation is functionally independent of the environmental parameters. As a consequence, a universal matrix

$$\boldsymbol{W} = \begin{bmatrix} w_{-N_s,-N_s} & \cdots & w_{-N_s,N_s} \\ \vdots & \ddots & \vdots \\ w_{N_s,-N_s} & \cdots & w_{N_s,N_s} \end{bmatrix} \in \mathbb{C}^{(2N_s+1)\times(2N_s+1)}$$

can be pre-canned into the system and used to spatially decorrelate primary data. Specifically, denoting by $\boldsymbol{Z}_P^c = [\boldsymbol{z}_{l_0-N_s}^c, \ldots, \boldsymbol{z}_{l_0}^c, \ldots, \boldsymbol{z}_{l_0+N_s}^c]$ the primary data matrix, we focus on the whitened primary data matrix given by $\boldsymbol{Z}_P = [\boldsymbol{z}_{l_0-N_s}, \ldots, \boldsymbol{z}_{l_0}, \ldots, \boldsymbol{z}_{l_0+N_s}] = \boldsymbol{Z}_P^c \boldsymbol{W}$. Following the same line of reasoning as for the primary data, it is also possible to come up with a set of decorrelated secondary data vectors free of the target returns, denoted by $\boldsymbol{r}_k$, $k = l_s+1, \ldots, l_s+K$, where $l_s \in \mathbb{N}$ is an integer indexing the first range cell containing interference only; it is clear that l_s accounts for a set of guard cells between primary and secondary data in order to make them statistically independent.

Summarizing, the decision problem to be solved can be formulated in terms of the following binary hypothesis test:

$$\begin{cases} H_0 : \begin{cases} \boldsymbol{z}_i &= \boldsymbol{n}_i, \\ & \quad i = l_0 - N_s, \ldots, l_0 + N_s, \\ \boldsymbol{r}_k &= \boldsymbol{n}_k, \\ & \quad k = l_s+1, \ldots, l_s+K, \end{cases} \\ \\ H_1 : \begin{cases} \boldsymbol{z}_i &= \alpha \mathcal{F}_i(\epsilon, \boldsymbol{W})\boldsymbol{v} + \boldsymbol{n}_i, \\ & \quad i = l_0 - N_s, \ldots, l_0 + N_s, \\ \boldsymbol{r}_k &= \boldsymbol{n}_k, \\ & \quad k = l_s+1, \ldots, l_s+K, \end{cases} \end{cases} \tag{3}$$

[1]Observe that $p(t)$ is a rectangular uncoded pulse.

[2]Notice that the sample under test is representative of a portion of the conventional range cell and hereafter l_0 denotes the *sub-bin under test*.

where α is the deterministic, but unknown, factor defined above; $\boldsymbol{v} \in \mathbb{C}^{N\times 1}$ is the nominal steering vector with $||\boldsymbol{v}|| = 1$ (for the sake of brevity we omit the dependence on ν and ν_s); $\boldsymbol{n}_i$, $i = l_0 - N_s, \dots, l_0 + N_s$, and $\boldsymbol{n}_k$, $k = l_s+1, \dots, l_s+K$, are independent and identically distributed complex normal random vectors with zero mean and covariance matrix $\boldsymbol{M} \in \mathbb{C}^{N\times N}$; finally,

$$\mathcal{F}_i(\epsilon, \boldsymbol{W}) = \sum_{m=-N_s}^{N_s} w_{m,i-l_0} \chi_p \left(mT_p/N_s - \epsilon, f \right),$$

$$-T_p/(2N_s) \le \epsilon \le T_p/(2N_s), \quad i = l_0 - N_s, \dots, l_0 + N_s.$$

In the next section we solve problem (3) resorting to the plain GLRT design procedure.

3. DETECTOR DESIGN

As a preliminary step towards the derivation of the receiver, we recall the expressions of the probability density function (pdf) of the whitened primary data $\boldsymbol{Z}_P$ under both hypotheses and that of the whitened secondary data $\boldsymbol{Z}_S = [\boldsymbol{r}_{l_s+1}, \cdots, \boldsymbol{r}_{l_s+K}]$. Under the above assumption, the pdf of $\boldsymbol{Z}_P$ is given by

$$f_1(\boldsymbol{Z}_P; \boldsymbol{M}, \alpha, \epsilon) = \left[\frac{1}{\pi^N \det(\boldsymbol{M})} \right]^{2N_s+1} \times \exp\left\{ -\mathrm{Tr}\left[\boldsymbol{M}^{-1} \sum_{i=l_0-N_s}^{l_0+N_s} \boldsymbol{u}_i(\alpha,\epsilon) \boldsymbol{u}_i^\dagger(\alpha,\epsilon) \right] \right\}$$

under H_1 and by

$$f_0(\boldsymbol{Z}_P; \boldsymbol{M}) = \left[\frac{1}{\pi^N \det(\boldsymbol{M})} \right]^{2N_s+1} \times \exp\left\{ -\mathrm{Tr}\left[\boldsymbol{M}^{-1} \sum_{i=l_0-N_s}^{l_0+N_s} \boldsymbol{z}_i \boldsymbol{z}_i^\dagger \right] \right\}$$

under H_0, where

$$\boldsymbol{u}_i(\alpha,\epsilon) = \boldsymbol{z}_i - \alpha \mathcal{F}_i(\epsilon, \boldsymbol{W}) \boldsymbol{v}, \quad i = l_0 - N_s, \dots, l_0 + N_s. \tag{4}$$

On the other hand, the pdf of $\boldsymbol{Z}_S$ has the following expression

$$f(\boldsymbol{Z}_S; \boldsymbol{M}) = \left[\frac{1}{\pi^N \det(\boldsymbol{M})} \right]^{K} \times \exp\left\{ -\mathrm{Tr}\left[\boldsymbol{M}^{-1} \sum_{i=l_s+1}^{l_s+K} \boldsymbol{r}_i \boldsymbol{r}_i^\dagger \right] \right\}.$$

Finally, let us define symbols that will come in handy for the mathematical derivations

$$\boldsymbol{S} = \sum_{i=l_s+1}^{l_s+K} \boldsymbol{r}_i \boldsymbol{r}_i^\dagger, \tag{5}$$

$$\boldsymbol{\mathcal{F}}(\epsilon) = \left[\mathcal{F}_{l_0-N_s}(\epsilon, \boldsymbol{W}), \dots, \mathcal{F}_{l_0+N_s}(\epsilon, \boldsymbol{W}) \right]^T, \tag{6}$$

$$-T_p/(2N_s) \le \epsilon \le T_p/(2N_s). \tag{7}$$

Given the independence between primary and secondary data, the GLRT for problem (3) is the following decision rule

$$\Lambda(\boldsymbol{Z}_P, \boldsymbol{Z}_S) = \frac{\max\limits_{\epsilon\in\mathcal{I}, \boldsymbol{M}, \alpha} f_1(\boldsymbol{Z}_P; \boldsymbol{M}, \alpha, \epsilon) f(\boldsymbol{Z}_S; \boldsymbol{M})}{\max\limits_{\boldsymbol{M}} f_0(\boldsymbol{Z}_P; \boldsymbol{M}) f(\boldsymbol{Z}_S; \boldsymbol{M})} \underset{H_0}{\overset{H_1}{\gtrless}} \eta, \tag{8}$$

where the expression of $f_1(\cdot;\cdot)$ depends on the value of ϵ and η is the threshold value set according to the desired probability of false alarm (P_{fa}). Hereafter η will denote any modification of the original threshold.

The following proposition summarizes the main contribution of this paper

Proposition 3.1 *Plain GLRT can be recast as*

$$\max_{\epsilon\in[-T_p/(2N_s)\; T_p/(2N_s)]} \frac{\det\left[\boldsymbol{I} + \boldsymbol{Z}_P^\dagger \boldsymbol{S}^{-1} \boldsymbol{Z}_P \right]}{\det\left[\bar{\boldsymbol{S}} \right]} \underset{H_0}{\overset{H_1}{\gtrless}} \eta, \tag{9}$$

where

$$\bar{\boldsymbol{S}} = \boldsymbol{I} + (\boldsymbol{Z}_P - \widehat{\alpha}(\epsilon)\boldsymbol{v}\boldsymbol{\mathcal{F}}(\epsilon)^T)^\dagger \boldsymbol{S}^{-1} (\boldsymbol{Z}_P - \widehat{\alpha}(\epsilon)\boldsymbol{v}\boldsymbol{\mathcal{F}}(\epsilon)^T),$$

with $\widehat{\alpha}(\epsilon)$ being the maximum likelihood estimate of α given by

$$\widehat{\alpha}(\epsilon) = \frac{\boldsymbol{v}^\dagger \boldsymbol{S}^{-1} \boldsymbol{Z}_P \left[\boldsymbol{I} + \boldsymbol{Z}_P^\dagger \boldsymbol{S}^{-\frac{1}{2}} \boldsymbol{P}_{\boldsymbol{v}_S}^\perp \boldsymbol{S}^{-\frac{1}{2}} \boldsymbol{Z}_P \right]^{-1} \boldsymbol{\mathcal{F}}(\epsilon)^*}{\boldsymbol{\mathcal{F}}(\epsilon)^T \left[\boldsymbol{I} + \boldsymbol{Z}_P^\dagger \boldsymbol{S}^{-\frac{1}{2}} \boldsymbol{P}_{\boldsymbol{v}_S}^\perp \boldsymbol{S}^{-\frac{1}{2}} \boldsymbol{Z}_P \right]^{-1} \boldsymbol{\mathcal{F}}(\epsilon)^* \boldsymbol{v}^\dagger \boldsymbol{S}^{-1} \boldsymbol{v}},$$

and

$$\boldsymbol{P}_{\boldsymbol{v}_S}^\perp = \boldsymbol{I} - \boldsymbol{S}^{-\frac{1}{2}} \boldsymbol{v}\boldsymbol{v}^\dagger \boldsymbol{S}^{-\frac{1}{2}} / (\boldsymbol{v}^\dagger \boldsymbol{S}^{-1} \boldsymbol{v}). \tag{10}$$

Maximization over ϵ cannot be conducted in closed form. Thus, we have to resort to a grid search to perform the optimization over ϵ. Any grid-search-based implementation of this detector will be referred to in the following as the oversampled GLRT (OS-GLRT). Remarkably, following the lead of [7] it is not difficult to show that the OS-GLRT ensures the CFAR property with respect to the interference covariance matrix $\boldsymbol{M}$.

4. PERFORMANCE ASSESSMENT

In this section, we analyze the performance of the proposed detection algorithm in terms of probability of detection and root mean square (RMS) error in range. To this end, we compare the proposed detector to the so-called modified Kelly's

GLRT (M-GLRT) and modified AMF (M-AMF) derived in [7]. For simulation purposes we make use of standard Monte Carlo counting techniques and evaluate the thresholds necessary to ensure a preassigned value of P_{fa} resorting to $100/P_{fa}$ independent trials. The P_d values and the RMS range errors are estimated over 10^4 and 500 independent trials, respectively.

The actual position of the target is generated (independent from trial to trial) uniformly distributed in $(t_{\min}+(l_0-1)T_p-T_p/(2N_s),\ t_{\min}+(l_0-1)T_p+T_p/(2N_s))$. Finally, all the illustrative examples assume a rectangular pulse of duration $T_p = 0.2\ \mu$s, $P_{fa} = 10^{-4}$, $f_c = 10^9$ Hz, $c = 3 \cdot 10^8$ m/s, and that ϵ takes on values in

$$\left\{ \frac{n - N_\epsilon}{2N_\epsilon} \frac{T_p}{N_s} \right\}_{n=0}^{2N_\epsilon} \tag{11}$$

with $N_\epsilon = 5$.

The interference is modeled as a complex normal vector with the following space-time covariance matrix

$$\boldsymbol{M} = \sigma_n^2 \boldsymbol{I}_N + \sigma_c^2 \boldsymbol{M}_t \otimes \boldsymbol{M}_s, \tag{12}$$

where $\otimes$ denotes the Kronecker product, $\sigma_n^2 = 1$, $\sigma_c^2 > 0$ is evaluated assuming a clutter-to-noise ratio of 30 dB, the (i,j)th element of $\boldsymbol{M}_s \in \mathbb{C}^{N_a \times N_a}$ is given by $\rho_s^{|i-j|}$ with $\rho_s = 0.9$, and the the (i,j)th element of $\boldsymbol{M}_t \in \mathbb{C}^{N_p \times N_p}$ is given by $\rho_t^{|i-j|}$ with $\rho_t = 0.9$.

Finally, given the actual value of ϵ, the SNR has the following expression

$$\text{SNR} = |\alpha|^2 \boldsymbol{v}^\dagger \boldsymbol{M}^{-1} \boldsymbol{v} \sum_{i=l_0-N_s}^{l_0+N_s} |\mathcal{F}_i(\epsilon, \boldsymbol{W})|^2. \tag{13}$$

In Figures 1 and 2, we compare the OS-GLRT with the M-GLRT and the M-AMF assuming $N = N_a = 8$, $K = 16$, and N_s as parameter. In particular, in Figure 1 we plot P_d versus SNR, while in Figure 2 the comparisons are in terms of RMS errors in range.

Inspection of Figure 1 highlights that the greater N_s the higher the gain of the OS-GLRT with respect to the M-GLRT and the M-AMF. Observe that when $N_s = 1$ the OS-GLRT coincides with the M-GLRT. The trend found in Figure 1 can be also observed in Figure 2, where the RMS errors in range decreases as N_s increases. Finally, it is worth noticing that for high SNR values such RMS errors are determined by the grid resolution $\Delta_\epsilon = T_p/(2N_sN_\epsilon)$ (with $N_\epsilon = 5$, $N_s = 2, 4$). In fact, a uniformly distributed random variable in $(-\Delta_r/2, \Delta_r/2)$ with Δ_r denoting the grid resolution in range, namely $\Delta_r = \Delta_\epsilon c/2$, has a standard deviation equal to $\Delta_r/\sqrt{12}$ that for the parameter values herein considered means a lower-bound on the RMS errors of 0.44 m for $N_s = 2$ and 0.22 m for $N_s = 4$.

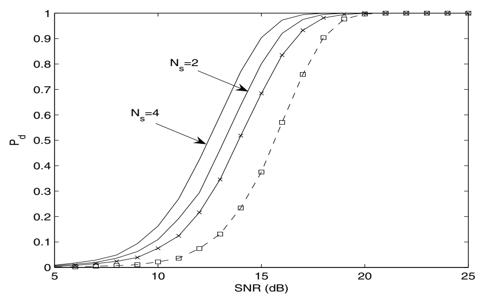

Fig. 1. P_d versus SNR for the OS-GLRT (no marker and solid line), the M-GLRT (cross marker and solid line), and the M-AMF (square marker and dashed line); $N = N_a = 8$, $K = 16$, $N_\epsilon = 5$, and $P_{fa} = 10^{-4}$.

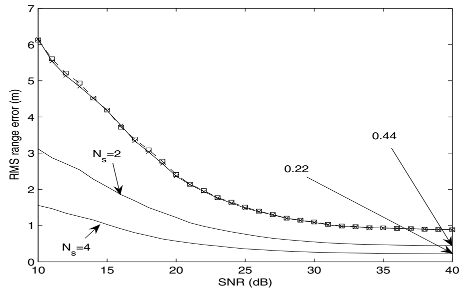

Fig. 2. RMS errors in range versus SNR for the OS-GLRT (no marker and solid line), the M-GLRT (cross marker and solid line), and the M-AMF (square marker and dashed line); $N = N_a = 8$, $K = 16$, $N_\epsilon = 5$, and $P_{fa} = 10^{-4}$.

5. CONCLUSION

In this work, we have attacked the problem of adaptive detection and range estimation of a point-like target buried in homogeneous Gaussian disturbance. At the design stage we have taken advantage of both oversampling of the noisy returns and target energy spillover to adjacent range samples to derive an adaptive receiver with enhanced localization capability. As customary, we have assumed that a set of secondary data, free of signal components and sharing the same spectral properties of the disturbance in the primary data, is available. Remarkably, the proposed decision scheme ensures the desirable CFAR property with respect to the unknown parameters of the interference. The performance assessment has shown that the oversampling yields superior performance in terms of both probability of detection and estimation accuracy of target position within the range bin. In fact, the OS-GLRT outperforms the M-GLRT and the M-AMF with a gain that grows as the oversampling factor increases.

6. REFERENCES

[1] E. J. Kelly, "An adaptive detection algorithm," *IEEE Transactions on Aerospace and Electronic Systems*, vol. 22, no. 2, pp. 115–127, March 1986.

[2] E. J. Kelly and K. Forsythe, "Adaptive detection and parameter estimation for multidimensional signal models," Tech. Rep. No. 848, Lincoln Lab, MIT, April 1989.

[3] Y. I. Abramovich, N. K. Spencer, , and A. Y. Gorokhov, "Modified glrt and amf framework for adaptive detectors," *IEEE Transactions on Aerospace and Electronic Systems*, vol. 43, no. 3, pp. 1017–1051, July 2007.

[4] F. Gini, A. Farina, and M. Greco, "Selected list of references on radar signal processing," *IEEE Transactions on Aerospace and Electronic Systems*, vol. 37, no. 1, pp. 329–359, January 2001.

[5] X. Zhang, P. K. Willett, and Y. Bar-Shalom, "Monopulse radar detection and localization of multiple unresolved targets via joint bin processing," *IEEE Transactions on Signal Processing*, vol. 53, no. 4, pp. 1225–1236, April 2005.

[6] X. Zhang, P. K. Willett, and Y. Bar-Shalom, "Detection and localization of multiple unresolved extended targets via monopulse radar signal processing," *IEEE Transactions on Aerospace and Electronics Systems*, vol. 45, no. 2, pp. 455–472, April 2009.

[7] D. Orlando and G. Ricci, "Adaptive radar detection and localization of a point-like target," *IEEE Transactions on Signal Processing*, vol. 59, no. 9, pp. 4086–4096, September 2011.

[8] J. R. Guerci, *Space-Time Adaptive Processing for Radar*, MA: Artech House, 2003.

[9] R.D. Brown, R.A. Schneible, M.C. Wicks, H. Wang, and Yuhong Zhang, "Stap for clutter suppression with sum and difference beam," *IEEE Transactions on Aerospace and Electronics Systems*, vol. 36, no. 2, pp. 634–646, April 2000.

[10] E. Conte, A. De Maio, and G. Ricci, "Glrt-based adaptive detection algorithms for range-spread targets," *IEEE Transactions on Signal Processing*, vol. 49, no. 7, pp. 1336–1348, July 2001.

[11] C. Hao, J. Yang, X. Ma, C. Hou, and D. Orlando, "Adaptive detection of distributed targets with orthogonal rejection," *IET Radar, Sonar and Navigation*, vol. 6, no. 6, pp. 483–493, July 2012.

[12] A. Aubry, A. De Maio, L. Pallotta, and A. Farina, "Radar detection of distributed targets in homogeneous interference whose inverse covariance structure is defined via unitary invariant functions," *IEEE Transactions on Signal Processing*, vol. 61, no. 20, pp. 4949–4961, October 2013.

[13] N. Levanon, *Radar Principles*, John Wiley & Sons, Inc., 1998.